**Advances in Nano Research**, *Vol. 10, No. 1 (2021) 77-90*
DOI: https://doi.org/10.12989/anr.2021.10.1.077



# Experimental design approach for ultra-fast nickel removal by novel bio-nanocomposite material

Olcay K. Ince[1,2], Burcu Aydogdu[3], Hevidar Alp[*2,4] and Muharrem Ince[2,5]

[1]*Department of Gastronomy and Culinary Arts, Faculty of Fine Arts, Design and Architecture, Munzur University, 62000 Tunceli, Turkey*
[2]*Rare Earth Elements Application and Research Center, Munzur University, 62000 Tunceli, Turkey*
[3]*Department of Mechanical Engineering, Faculty of Engineering, Munzur University, 62000 Tunceli, Turkey*
[4]*Department of Food Process, Tunceli Vocational School, Munzur University, 62000 Tunceli, Turkey*
[5]*Department of Chemistry and Chemical Processes, Tunceli Vocational School, Munzur University, 62000 Tunceli, Turkey*

(*Received November 6, 2019, Revised September 21, 2020, Accepted October 16, 2020*)

**Abstract.** In the present study, novel chitosan coated magnetic magnetite ($Fe_3O_4$) nanoparticles were successfully biosynthesized from mushroom, *Agaricus campestris*, extract. The obtained bio-nanocomposite material was used to investigate ultra-fast and highly efficient for removal of $Ni^{2+}$ ions in a fixed-bed column. Chitosan was treated as polyelectrolyte complex with $Fe_3O_4$ nanoparticles and a Fungal Bio-Nanocomposite Material (FBNM) was derived. The FBNM was characterized by using X-Ray Diffractometer (XRD), Scanning Electron Microscopy-Energy Dispersive X-Ray Spectroscopy (SEM-EDS), Fourier Transform Infrared spectra (FTIR) and Thermogravimetric Analysis (TGA) techniques and under varied experimental conditions. The influence of some important operating conditions including pH, flow rate and initial $Ni^{2+}$ concentration on the uptake of $Ni^{2+}$ solution was also optimized using a synthetic water sample. A Central Composite Design (CCD) combined with Response Surface Modeling (RSM) was carried out to maximize $Ni^{2+}$ removal using FBNM for adsorption process. A regression model was derived using CCD to predict the responses and analysis of variance (ANOVA) and lack of fit test was used to check model adequacy. It was observed that the quadratic model, which was controlled and proposed, was originated from experimental design data. The FBNM maximum adsorption capacity was determined as 59.8 mg $g^{-1}$. Finally, developed method was applied to soft drinks to determine $Ni^{2+}$ levels. Reusability of FBNM was tested, and the adsorption and desorption capacities were not affected after eight cycles. The paper suggests that the FBNM is a promising recyclable nanoadsorbent for the removal of $Ni^{2+}$ from various soft drinks.

**Keywords:** *Agaricus campestris*; $Fe_3O_4$ nanoparticles; bionano-composite material; nickel; fixed-bed column

## 1. Introduction

The biggest pollutants encounter the world are heavy metals. Heavy metals damaged the environment and human health in many aspects. Since toxic metals are used in many fields of industry, without discharge of their release to the environment is also increasing. Heavy metals, which spread to the environment and do not degrade, reach people especially through the food chain and water (Ince and Kaplan Ince 2019a, Pala *et al*. 2019, Serdar *et al*. 2019). Therefore, the determination of the heavy metals amount in food and water samples is important issue for human health (Qin *et al*. 2012). The $Ni^{2+}$ is one of these heavy metals, which has many harmful effects to the environment and human health and is used in many fields of industry (electroplating, mineral processing, batteries, paint, etc.) (Bhatnagar and Minocha 2010, Mondal *et al*. 2017). The Ni compounds lead health problems when accumulate in human body, including lung diseases, respiratory failure, cardiovascular diseases, birth defects, asthma, chronic bronchitis, gastrointestinal distress, pulmonary fibrosis and renal edema, allergic reactions (Denkhaus and Salnikow 2002, Boujelben *et al*. 2009, Hanafiah *et al*. 2010, Katsou *et al*. 2010, Bhatnagar and Minocha 2010). The World Health Organization (WHO) limited permissible concentration of nickel in drinking water as 0.01 mg $L^{-1}$ (Kadirvelu *et al*. 2001, Sharma and Singh 2013). Because of all these negative effects, all heavy metals, especially $Ni^{2+}$, must be removed before discharged. For removal of these metals a number of techniques including ion exchange process (Smara *et al*. 2007), organic-based ligand precipitation (Esalah and Husein 2008), membrane and reverse osmosis processes (Mohsen-Nia *et al*. 2007, Landaburu-Aguirre *et al*. 2010) have been used. These methods are of limited use, due to high expense and operational costs (Pacheco *et al*. 2006, Garg *et al*. 2008). Because of these disadvantages of other methods, it is preferred to use adsorption technique. The aim of the developed adsorption studies is to use materials that will not harmful to environment and to reduce the cost. For this reason, spontaneous and abundant substances are used in nature as live biomass or live biomass wastes (Ince 2014, Kaplan Ince *et al*. 2017, Ince *et al*. 2017, Ince and Kaplan Ince 2017) and clay (Kaplan Ince *et al*. 2018). With the development of technology, magnetic nanoparticles have been used various applications and also

*Corresponding author, Ph.D., Assistant Professor,
E-mail: halp@munzur.edu.tr



ISSN: 2287-237X (Print), 2287-2388 (Online)

as adsorbent. Due to higher surface area, accordingly, the high adsorption capacity, greater active sites for interaction with metallic species, and can be synthesized from many different materials (Padmavathy *et al*. 2003, Mak and Chen 2005, Lee and Harris 2006, Haddad *et al*. 2008, Hritcu *et al*. 2009, Hepziba Suganthi and Kandasamy 2017). Besides all these advantages, they can be used in many application fields as mineral separation, magnetic storage devices, catalysis, magnetic refrigeration system, heat transfer application in drug delivery system, magnetic resonance imaging, cancer therapy, and magnetic cell separation (Liu *et al*. 2004, Hu *et al*. 2006, Zhou *et al*. 2007, Sharma *et al*. 2009, Teja and Koh 2009, Sharma and Srivastava 2010). Furthermore, magnetic separation is emerging as easy and economical method for sorbent recovery by applying an external magnetic field (Wang *et al*. 2010, Mohan *et al*. 2011). Magnetite, a ferrite compound which has a cubic inverse spinel structure, has been frequently carried out for magnetic separation due to its electric and magnetic properties owing to the electronic transfer in the octahedral sites between $Fe^{2+}$ and $Fe^{3+}$ (Chen *et al.* 2006). Also, magnetite is chemically stable, biocompatible, not toxic and hydrophilic so these nanoparticles used in biology, chemistry, medicine, physics and various engineerings (Chen *et al*. 2006, Gu *et al*. 2006, Li *et al*. 2008, Hu *et al*. 2009). Metal removal from many sources has always been the focus of interest from past to present. Therefore, new techniques and adsorbents are being developed for metal removal. In this study, a novel reusable nano-adsorbent was produced and used. Magnetite nanoparticles' surface was functionalised and modificated with chitosan and the obtained magnetic chitosan/$Fe_3O_4$ composites were used as nano-adsorbent to remove $Ni^{2+}$ ions from soft drinks. This study is important in terms of the source of material that used to obtain nanoparticles. Magnetite nanoparticles were derived from a mushroom, *Agaricus campestris*, extract. Continuous-flow fixed-bed columns are more preferable than batch operation systems for metal removal in practical processes (Chu 2004). When metal solution is introduced into a fixed-bed column, metal ions load onto the top of adsorbents and flow through the packed bed. A proper design of fixed-bed column adsorption system is essential to provide basic data for many applications especially industrial application (Pan *et al*. 2005). Adsorption is frequently performed in a continuous fixed-bed column system (Volesky 2001), due to its proper size and mechanical strength, which is imperative for a large-scale treatment of industrial wastewater (Qu *et al*. 2019). To evaluate FBNM $Ni^{2+}$ removal efficiency, column process variables need to be optimized. Conventional techniques are not preferred because a great number of experiments are needed. Instead of conventional techniques, a statistical experimental design approach preference is more advantageous. The major disadvantage of these methods is that the interaction between the process variables on the dependent variable cannot be determined. Such a problem can be overcome by using a statistical experimental design, which not only reduces the number of experiments but also provides an appropriate model for process optimization, which helps to evaluate the effects between the variables. In recent years, different experimental design methods have been preferred for multivariate physicochemical process optimization (Ince and Kaplan Ince 2017, 2019a, Kaplan Ince *et al*. 2018). Especially, RSM, is a useful tool, has been used to understand effect of several variables influencing the responses by varying them simultaneously and carrying out a limited number of experiments. In this study, a novel FBNM was successfully biosynthesized and applied to soft drinks to investigate adsorbent efficiency for the removal of $Ni^{2+}$ ions in a fixed-bed column. Although batch experiments are used to obtain equilibrium sorption isotherms and to evaluate the sorption capacity of sorbents for several metals, in the practical operation of full-scale biosorption processes, continuous-flow fixed-bed columns are often preferred (Fonseca *et al*. 2009). As a result, it is difficult to carry out a prior design and optimization of fixed-bed columns without a quantitative approach (Miralles *et al*. 2010). Over the last few years there are numerous studies about metals removal using various materials by batch adsorption technique. However, there is only limited research on the preparation of nanoparticles

Table 1 Experimental factors and levels in the CCD

| Factors | Levels | | | Star point $\alpha = 2$ | |
|---|---|---|---|---|---|
| | Low (−1) | Central (0) | High (+1) | $-\alpha$ | $+\alpha$ |
| ($X_1$) pH | 3 | 5.5 | 8 | 0.5 | 10.5 |
| ($X_2$) Flow rate (mL $min^{-1}$) | 2 | 3 | 4 | 1 | 5 |
| ($X_3$) Initial concentration (mg $L^{-1}$) | 30 | 40 | 50 | 20 | 60 |

| Run | $X_1$ | $X_2$ | $X_3$ | mg Ni $g^{-1}$ FBNM |
|---|---|---|---|---|
| 1 | 5.5 | 5 | 40 | 32.44 |
| 2 | 8 | 2 | 30 | 17.76 |
| 3 | 5.5 | 3 | 20 | 10.57 |
| 4 | 5.5 | 3 | 40 | 47.28 |
| 5 | 10.5 | 3 | 40 | 0.1 |
| 6 | 5.5 | 3 | 40 | 46.56 |
| 7 | 5.5 | 3 | 60 | 55.8 |
| 8 | 3 | 4 | 50 | 41.08 |
| 9 | 5.5 | 1 | 40 | 36.4 |
| 10 | 3 | 4 | 30 | 10.32 |
| 11 | 5.5 | 3 | 40 | 55.84 |
| 12 | 8 | 4 | 50 | 31.56 |
| 13 | 5.5 | 3 | 40 | 52.3 |
| 14 | 3 | 2 | 30 | 13.48 |
| 15 | 3 | 2 | 50 | 38.8 |
| 16 | 5.5 | 3 | 40 | 54.4 |
| 17 | 0.5 | 3 | 40 | 3.24 |
| 18 | 8 | 4 | 30 | 14.24 |
| 19 | 8 | 2 | 50 | 33.3 |
| 20 | 5.5 | 3 | 40 | 54.2 |

and its column application for removing $Ni^{2+}$ ions from various drinks. As a result, the aims of present study can be summarized as follows: (1) To obtain maximum adsorption capacity of FBNM by using a CCD optimization approach; (2) to investigate four independent variables effect on $Ni^{2+}$ adsorption and their interactions for $Ni^{2+}$ removal; (3) to verify the validity of the proposed model by using ANOVA; (4) to optimize column conditions; and (5) to apply the developed method to real samples for determination of $Ni^{2+}$ ions' levels.

## 2. Experimental

### *2.1 Chemicals and instruments*

Nickel solution, sodium hydroxide and hydrochloric acid were purchased from Merck company (Darmstadt, Germany). The $FeCl_2.4H_2O$ and $FeCl_3.6H_2O$ were purchased from Sigma-Aldrich (USA). All used chemicals were of commercially available analytical grade. The FBNM and $Ni^{2+}$ loaded FBNM were characterized using Fourier Transform Infrared (FTIR) spectra, FTIR spectrophotometer with Attenuated Total Reflectance (ATR; 67000, Japan). Surface morphology and X-ray analysis of FBNM and $Ni^{2+}$ loaded FBNM were performed using a digital Scanning Electron Microscopy (SEM) coupled with Energy Dispersive X-Ray Spectroscopy (EDS; Hitachi SU3500, Japan) and X-Ray Diffractometer (XRD; Rigaku MiniFlex-600, Japan), respectively. The $Ni^{2+}$ ions concentrations were measured by Flame Atomic Absorption Spectrometer (FAAS) (Analyst™ 800, PerkinElmer, Inc., Shelton, CT, USA). To optimize flow rate in column system a Shenchen peristaltic pump (Wertheim-Germany) was used. Ultrapure water was used throughout experiment (ELGA LabWater/VWS; UK). An EZDO bench top PL-700 PV model pH-meter was used pH measurements for fixed-bed column experiments.

### *2.2 Preparation of mushroom extract*

The mushroom (*Agaricus campestris*) collected from the Pülümür region of Tunceli-Turkey and then they were washed and dried in a drying oven for 48 h at 40°C before being used. The dried mushroom samples were floured with muller and then sieved. The powdered samples were stored in glass jars and stored in a refrigerator at +4°C. Then the samples were weighed (5 g) for extraction and the powdered mushroom samples were placed in the flask and 100 mL of distilled water were added, followed by extraction for 72 hours at a stirring speed of 250 rpm at 40°C in shaking water bath. Then filtered and centrifuged at 6000 rpm. The supernatants were stored to check whether they contained iron nanoparticles.

### *2.3 Biosynthesis of fungal $Fe_3O_4$ nanoparticles*

For the biosynthesis, initially a mixture solution was prepared by taking 0.25 M of $FeCl_2$ and 0.5 M of $FeCl_3$ in 250 mL of distilled water and heated to 80°C with stirring at 250 rpm. After 10 minutes, 250 mL of fungal extract were added. After 5 minutes, 1 M NaOH was added dropwise at a rate of 7 mL $min^{-1}$ and the reddish-brown mixture was converted to black suspended particles confirming the biosynthesis of fungal $Fe_3O_4$ nanoparticles. After completion of the reaction, the reaction mixture was allowed to cool to room temperature. Fungal magnetic $Fe_3O_4$ nanoparticles separated using centrifugation at 6000 rpm for 10 min. Homogeneous magnetite particles were collected, dried in the oven and stored at room temperature for further characterization and hydrogel coatings.

Nanoparticles synthesized by biological resources such as bacteria, fungus, animals and plants can be synthesized in laboratories in recent studies. This is called green synthesis. Balaz *et al*. (2019) synthesized silver nanoparticles using green approach from the *Origanum vulgare* L. plant water extract. They studied five different concentrations of the silver nitrate precursor and they found that the concentration was low, the synthesis was very fast. The antibacterial activity was pursued using five different concentrations of the silver nitrate precursor. The positive correlation between the grain size distribution and antibacterial activity was found out by them. Supraja *et al*. (2018) used aqueous extract of *Sargassum muticum* which is brown algae for synthesized silver nanoparticles (AgNPs) for antimicrobial and anticancer efficacy. They indicated that the synthesized AgNPs was a strong antimicrobial activity against bacteria and effective anticancer activity against Breast cancer cell line. Punjabi *et al*. (2018) synthesized silver nanoparticles using *Pseudomonas hibiscicola* that isolated from an electroplating industry in Mumbai. They emphasized that proteins in extracellular secretion correlated with synthesized of nanoparticles in this study. Malarkodi *et al*. (2013) synthesized cadmium sulfide nanoparticles (CdSNPs) as semiconductor nanoparticles from the reduction of cadmium sulphate solution, using the bacteria of *Serratia nematodiphila*. They reported that the cadmium sulfide nanoparticles exhibited good bactericidal activity against *Bacillus subtilis*, *Klebsiella planticola*.

### *2.4 Preparation of fungal bio-nanocomposite material (FBNM)*

About 1 g of chitosan in 1% acetic acid solution was stirred at 750 rpm for 2 hours until homogeneous. Then, 1 g of fungal $Fe_3O_4$ was added and stirred for a further 4 hours until homogeneous. The homogeneous solution prepared by syringe was then added to a 1 M NaOH solution at a rate of 2 mL $min^{-1}$. Obtained FBNM beads were filtered and washed at least three times with ultra-pure water. After some of the FBNM were prepared and filled in a fixed-bed column for $Ni^{2+}$ ions removal from some soft drinks, the remaining FBNM were dried and stored at room temperature for characterizations. Bhagawati *et al*. (2016) procreated a low cost castor oil based hyperbranched/ bitumen modified fly ash nanocomposite as a surface coating material and this study predicated that these nanocomposites may be used as environment friendly surface coating materials.

### 2.5 Preparation of the column and adsorption-desorption studies

A polyethylene column was filled with about 25 mg FBNM material for solid phase extraction. Firstly, 10 mL ultra-pure water was passed through the column in order to condition and clean it before use. The influence of important operating conditions including pH (3-8), flow rate (2-4 mL $min^{-1}$) and initial $Ni^{2+}$ ions concentration (30-50 mg $L^{-1}$) on the uptake of $Ni^{2+}$ solution was identified by using CCD and model solution was passed through the prepared column at an adjusted flow rate with a peristaltic pump. The retained $Ni^{2+}$ on the FBNM was then eluted with using procedure that is explained in the sample preparation step. Finally, the $Ni^{2+}$ concentrations in this solution was measured by FAAS.

### 2.6 Preparation of soft drinks

Concentrated nitric acid (3 mL of concentrated nitric acid was used for 50 mL of sample) was added to soft drink samples and were degassed using an ultrasonic bath at 40ºC about 30 min prior to analysis (Eticha and Hymete 2014). After acidification and degassing process, to prevent contamination, samples were placed into 250 mL glass beakers and covered with watch glasses in order. Then, the optimized method was applied to each sample. All samples were passed the column. Then, column filler material was treated with 1 mL 0.1 M of hydrochloric acid. Analytical blanks were prepared in a similar manner. All samples and blanks were analyzed for $Ni^{2+}$ concentration using FAAS equipped with deuterium arc background corrector. All the samples were analyzed in triplicate.

### 2.7 Analytical method

An experiment process that is ultra-fast and highly efficient was performed to achieve $Ni^{2+}$ ions from soft drinks. Using Ni standard solutions with known concentrations from 0.1 to 2 mg $L^{-1}$ a calibration curve was created to calculate adsorbed $Ni^{2+}$ before the real samples' concentrations were determined. About 25 mg FBNM was filled the column and 50 mL of $Ni^{2+}$ solutions of initial concentrations (20-40 mg $L^{-1}$) pH (range from 3 to 7) was adjusted with (0.01-0.1 N) HCl and (0.01-0.1 N) NaOH. Solutions were passed the column using a peristaltic pump. After the end of the working, the column filling material was desorbed by 1 mL 0.1 M of hydrochloric acid and they were measured by FAAS. Adsorbed $Ni^{2+}$ amount by the unit mass of bio-nanocomposite material was calculated using the following Eq. (1)

$$q = \frac{(Co - Ce)\,V}{m} \tag{1}$$

where $q$ (mg $g^{-1}$), $C_e$ and $C_0$ represent amount adsorbed per gram of bio-nanocomposite material, equilibrium concentrations and $Ni^{2+}$ solution initial concentration (mg $L^{-1}$), respectively. Similarly, $m$ represents used bio-nanocomposite material mass and $V$ (L) refers to the initial concentration of $Ni^{2+}$ solution.

### 2.8 Experimental design and process optimization

The RSM is a collection of statistical and mathematical techniques useful for analyzing the effects of several independent variables on the response. This method is known as regression analysis and is used to obtain data, estimate parameters and establish relationships between test indexes and continuous variables (Ince and Kaplan Ince 2019b).

The use of design of experiments has boomed over the past decade. Indeed, their application covers all areas: food industry, chemicals, pharmaceuticals, etc. The goal is to study the effect of two or more parameters (called factors) on one (or more) response that we would to optimize with a high precision. This must be conducted with minimal testing to optimize time and resources required (Kaplan Ince *et al*. 2018, Pala *et al*. 2019).

In this respect, experimental designs are techniques to study the effects of different factors and optimize them in the experimental defined domain. It allows determining the statistically significant parameters that affects the responses studied. A series of tests is then achieved by varying the factors to obtain optimal response with respect to the criteria determined by the researchers (Bakraouy *et al*. 2017, Alp *et al*. 2019).

In this study, three factors with five-levels CCD was chosen to study and optimize the influence of process variables. Because the CCD experimental design basically involves three major steps, performing the statistically designed experiments, estimating the coefficients in a mathematical model, and predicting the response and checking the adequacy of the model. To measure the influence of each independent variables including pH ($X_1$), flow rate ($X_2$) and initial concentration ($X_3$) on $Ni^{2+}$ adsorption by FBNM a CCD experimental design (Table 1) was chosen.

The levels of variables were defined as low, medium and high with coded values of −1, 0 and +1, respectively. For each set of experiments, the star points of +2 and −2 were defined corresponding to α and $-\alpha$, respectively. By using this design, the main, interaction and quadratic effects of variables are modeled. This experimental design was conducted to minimize the effects of uncontrolled parameters and based on controllable factors. To optimize process variables and their interactions may be estimated by performing a minimum number of experiments but with an experimental design created with CCD. Also, optimization procedure ensures some advantages such as checking of model adequacy, response predicting besides mathematical model coefficients estimation (Ince and Kaplan Ince 2019b). This model determines both to examine the response to the maximum area of all variables and to identify the optimum value region. According to preliminary experiment studies, three critical parameters affecting $Ni^{2+}$ adsorption were selected as independent variables, adsorption of $Ni^{2+}$ ions on FBNM (Y) was considered as the dependent variable. In addition, to express the relationship between independent variables and

Table 2 Analysis of variance (ANOVA) for response surface quadratic model

| Source | Sum of squares | df | Mean square | F value | *p*-value Prob > F | |
|---|---|---|---|---|---|---|
| Model | 80.50 | 9 | 8.94 | 96.55 | < 0.0001 | significant |
| A-pH | 0.61 | 1 | 0.61 | 6.54 | 0.0285 | |
| B-flow rate | 0.15 | 1 | 0.15 | 1.62 | 0.2325 | |
| C-initial concentration | 19.34 | 1 | 19.34 | 208.82 | < 0.0001 | |
| AB | 0.012 | 1 | 0.012 | 0.13 | 0.7222 | |
| AC | 0.69 | 1 | 0.69 | 7.48 | 0.0210 | |
| BC | 0.11 | 1 | 0.11 | 1.16 | 0.3067 | |
| $A^2$ | 59.13 | 1 | 59.13 | 638.35 | < 0.0001 | |
| $B^2$ | 2.77 | 1 | 2.77 | 29.92 | 0.0003 | |
| $C^2$ | 5.27 | 1 | 5.27 | 56.93 | < 0.0001 | |
| Residual | 0.93 | 10 | 0.093 | | | |
| Lack of fit | 0.55 | 5 | 0.11 | 1.45 | 0.3476 | not significant |
| Pure error | 0.38 | 5 | 0.076 | | | |
| Cor total | 81.42 | 19 | | | | |
| R-squared | 0.9886 | | | | | |
| Adj R-squared | 0.9784 | | | | | |
| Pred R-squared | 0.9373 | | | | | |
| Adeq precision | 32.018 | | | | | |

*$p < 0.01$ highly significant; $0.01 < p < 0.05$ significant; $p > 0.05$ not significant

responses, experimental data were fitted to a second-order polynomial mathematical equation (Eq. (2)) and presented as below

$$Y(\text{mgNi /gFBNM}) = -0.73 + 0.64X_1 - 6.73X_2 + 0.09X_3 + 0.04X_4 - 3.45X_1X_2 - 3.26X_1X_3 - 1.05E - 0.03X_1X_4 - 5.19E - 0.04X_2X_3 - 5.53X_2X_4 + 1.14E - 0.03X_3X_4 - 0.02X_1^2 + 2.36X_2^2 - 1.01X_3^2 - 2.24E - 0.04X_4^2 \quad (2)$$

In the optimization of $Ni^{2+}$ ions adsorption on FBNM process to determine the optimum point and achieve highest treatment performance the best method is layout of the surface plot. Under predicted optimal conditions by using experiments that are identify by CCD, optimization results were verified. Predicted values of model that confirms RSM efficiency were strictly similar to results of corresponding experiments. According to obtained data from CCD experimental design, it can be said that CCD is the ideal approach to optimize the experimental variables when it used for $Ni^{2+}$ ions removal from some soft drinks by FBNM. It is a good evidence that the difference between the experimental and predicted results can be ignored both proposed quadratic models' efficiency and in predicting the optimum conditions. For optimum $Ni^{2+}$ ions adsorption numerical optimization values were obtained as 5.5 for pH, 2.5 mL $min^{-1}$ for flow rate and 49.5 mg $L^{-1}$ for $Ni^{2+}$ ions initial concentration. Independent variables experimental range and their levels for $Ni^{2+}$ ions adsorption on FBNM were showed in Table 1. Using the Design Expert software program (Design Expert Version 10, Stat-Ease, USA) a regression model was derived and proposed. Used parameters such as variable conditions, experimental values, and predicted values were presented in Table 2. Diagnostic checking tests provided by ANOVA were used for proposed model adequacy. In addition, chosen factors by quadratic models can be simply related to responses. Determination coefficient of $R^2$ characterizes the appropriate polynomial model. Because $R^2$ values, in the observed response values, provide a measure of how variability can be clarified by experimental factors and their interactions (Ince and Kaplan Ince 2017). Fisher's 'F'-test and *p*-value perform these analyzes.

## 3. Results and discussion

In literature, nanoparticles were produced by various techniques, materials and functionalized with various chemicals as, by bounding N-sodium acrylate-O-carboxymethyl chitosan [CMCH-g-PAA(Na)] on $Fe_3O_4$ nanoparticles (Asgari *et al*. 2014), functionalizing chitosan composite with EDTA (Chen *et al*. 2019), crosslinking hydrogel and chitosan on carboxymethyl-*β*-cyclodextrin (CM-*β*-CD) polymer modified $Fe_3O_4$ (Ding *et al*. 2015), functionalizing magnetic gold nanoparticles ($Fe_3O_4$ Au NPs) with thiol-terminated polyethylene glycol (Elbialy *et al*. 2014), by compositing graphene sheet with ferro ferric oxide and prepared graphene magnetic material (Guo *et al*. 2014), by bounding chitosan on magnetic $Fe_3O_4$ (Li *et al*. 2008, Yuwei and Jianlong 2011), xanthated $Fe_3O_4$-chitosan grafted onto graphene oxide (Liu *et al*. 2016), coating $Fe_3O_4$ by polymerized-chitosan (Ding *et al*. 2015), coating $Fe_3O_4$ by carboxymethyl chitosan (Zinadini *et al*. 2014), coating $Fe_3O_4$ with chitosan and functionalized with folate-poly(ethylene glycol)-COOH (Zhou *et al*. 2014), coating $Fe_3O_4$ nanoparticles with fucanpolysaccharides (Silva *et al*. 2013).

### *3.1 Characterization of bio-nanocomposite material*

#### *3.1.1 FTIR analysis*

Spectra of the pretreated FBNM and $Ni^{2+}$ ions loaded FBNM were compared (Fig. 1) by using FTIR. The spectra were recorded in the frequency range of 4000-500 $cm^{-1}$. Fig. 1 shows the changes and shifts in the FTIR bands during $Ni^{2+}$ ions adsorption on the FBNM. Major changes because of a strong band were observed in the region 3352-3289 $cm^{-1}$ corresponds to N-H and O-H stretching, as well as the intramolecular hydrogen bonds. Other changes and shifts can be summarized as follows: The absorption bands at around 2921 $cm^{-1}$ and 2868 $cm^{-1}$ can be attributed to C-H symmetric and asymmetric stretching, respectively. The presence of residual N-acetyl groups was confirmed by the

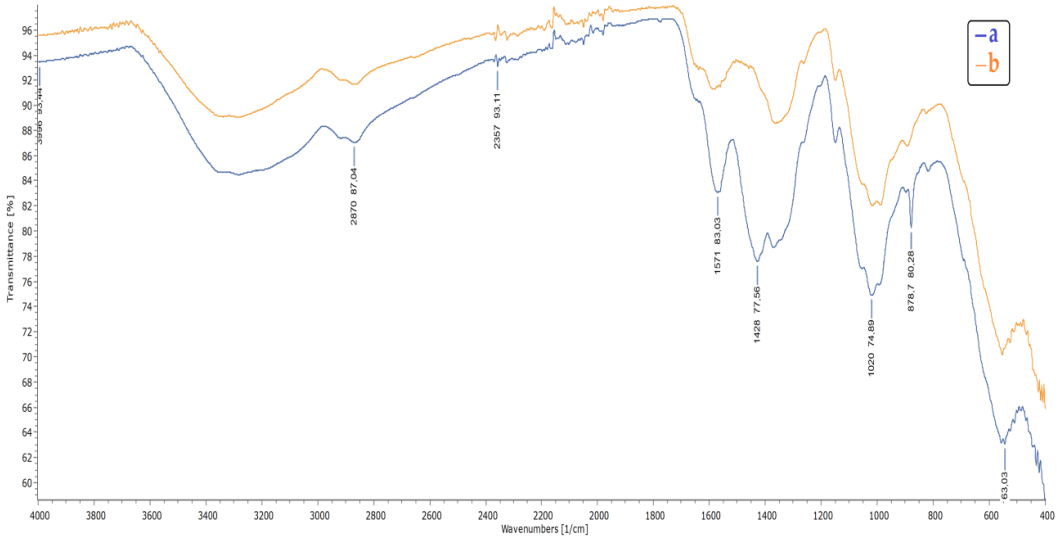


Fig. 1 FTIR spectra of FBNM and $Ni^{2+}$ ions-loaded FBNM

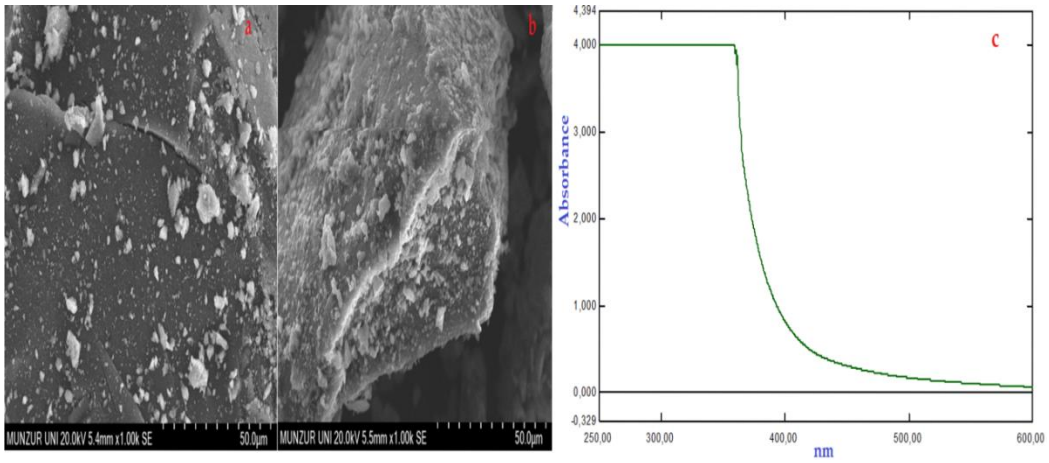


Fig. 2 SEM images of FBNM: (a) before adsorption of $Ni^{2+}$ ions; (b) after adsorption of $Ni^{2+}$ ions; (c) UV-Vis peaks $Fe_3O_4$ nanoparticles

bands at around 1648 $cm^{-1}$ (C=O stretching of amide I) and 1318 $cm^{-1}$ (C-N stretching of amide III), respectively. A band at 1588 $cm^{-1}$ corresponds to the N-H bending of the primary amine. The $CH_2$ bending and $CH_3$ symmetrical deformations were confirmed by the presence of bands at around 1416 $cm^{-1}$ and 1375 $cm^{-1}$, respectively. The absorption band at 1148 $cm^{-1}$ can be attributed to asymmetric stretching of the C-O-C bridge. The bands at 1059 $cm^{-1}$ and 1023 $cm^{-1}$ correspond to C-O stretching. The signal at 889 $cm^{-1}$ corresponds to the CH bending out of the plane of the ring of monosaccharides. The biosynthesized FBNM sample showed lower intensity peaks compared with the $Ni^{2+}$ ions loaded FBNM sample, suggesting a disruption of some of these groups during treatment.

### *3.1.2 SEM analysis*

To characterize the surface morphology and fundamental physical properties of the nano-adsorbent surfaces SEM micrographs has been a primary tool. They are useful to observe appropriate size distribution, porosity and particle shape of adsorbent. By using SEM, the morphological differences between the bio-nanocomposite material that called as FBNM and $Ni^{2+}$ ions loaded FBNM were evidenced for observing the appropriate size distribution, porosity and particle shape of adsorbents. These micrographs indicated that surface alterations in the FBNM morphology before and after $Ni^{2+}$ ions loading, and UV-Vis peak of $Fe_3O_4$ nanoparticles was presented in Fig. 2.

After being pretreated with $Ni^{2+}$ ions, surface of FBNM became rougher; this may be due to the $Ni^{2+}$ ions sorption onto FBNM. Based on these results it can be said that FBNM is a good adsorbent for adsorption of $Ni^{2+}$ ions. In addition, mineralogical composition of FBNM and $Ni^{2+}$ ions loaded FBNM were determined using EDS and shown at Fig. 3.

### *3.1.3 TGA analysis*

Thermogravimetric Analysis (TGA) of FBNM and $Ni^{2+}$ ions loaded FBNM were recorded in the temperature range of 30˚C-800˚C. It is observed that chitosan decomposition takes place in the temperature range of 242.1˚C-300˚C. On

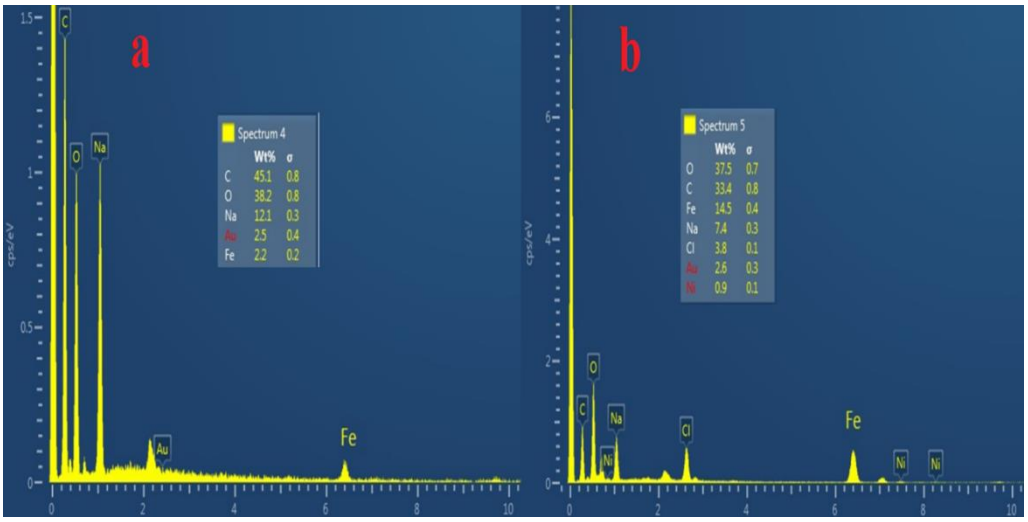


Fig. 3 EDS diagrams of FBNM: (a) before adsorption of $Ni^{2+}$ ions; (b) after adsorption of $Ni^{2+}$ ions

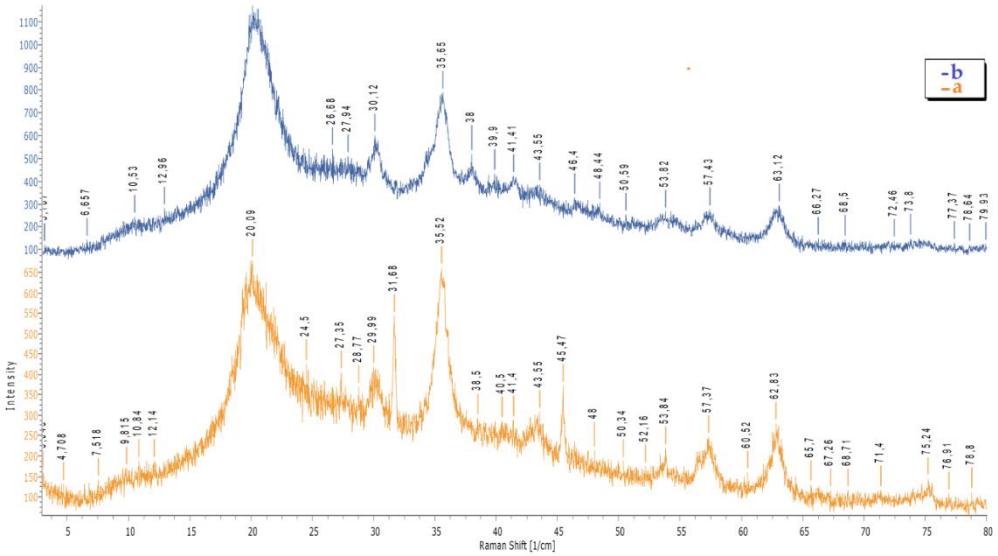


Fig. 4 EDS diagrams of FBNM: (a) before adsorption of $Ni^{2+}$ ions; (b) after adsorption of $Ni^{2+}$ ions

the other hand, $Ni^{2+}$ ions decomposition takes place in the temperature range of 300˚C-681.2˚C. From this analysis, it is observed that $Ni^{2+}$ ions loaded FBNM shows very similar degradation to FBNM. From TGA analysis, it is found that Ni loaded FBNM has a high thermal stability. Also based on TGA analysis it is very clear that no significant change was observed in the decomposition temperature of $Ni^{2+}$ ions and $Ni^{2+}$ ions loaded FBNM.

### *3.1.4 XRD analysis*

Fig. 4 presents the XRD of FBNM and $Ni^{2+}$ ions loaded FBNM, respectively. Since the XRD pattern is short-range, two chitosan signals are not expected since only two broad and weak reflections can be attributed to the amorphous structure. Six characteristic peaks for magnetite ($2\theta$ = 30.12°, 35.65°, 43.55°, 53.82°, 57.43° and 63.12°) and where the densest line is present in the XRD model (35, 67°) which were assigned to crystal planes of (220), (311), (400), (422), (511) and (440) planes of the iron oxide, respectively. The XRD showed peak around 20.5° in chitosan, which corresponded to 110 reflections (Shanmugapriya *et al*. 2011). $Ni^{2+}$ ions loaded magnetic particles show some variation in peak sharpness, and two different peaks were also seen in 31.68° and 45.47°.

The crystallite sizes of the nanocomposite are calculated using Debye-Scherrer formula (Eq. (3))

$$D = K\lambda/\beta \cos \tag{3}$$

where $D$ is the mean diameter of bio-nanoparticles, $\lambda$ is the X-ray wavelength ($\lambda = 1.54$ nm), $K = 0.94$ is the shape factor, $\theta$ is Bragg's angle, $\beta$ is the full width at half-maximum value of the respective XRD diffraction peak (Tsega and Dejene 2017). The average crystallite size of bio-nanocomposites was found to be in 8.02 nm and 7.27 nm. These results clearly revealed that the bio-nanocomposite size increased the radius of the crystal slightly by the effect of nickel.

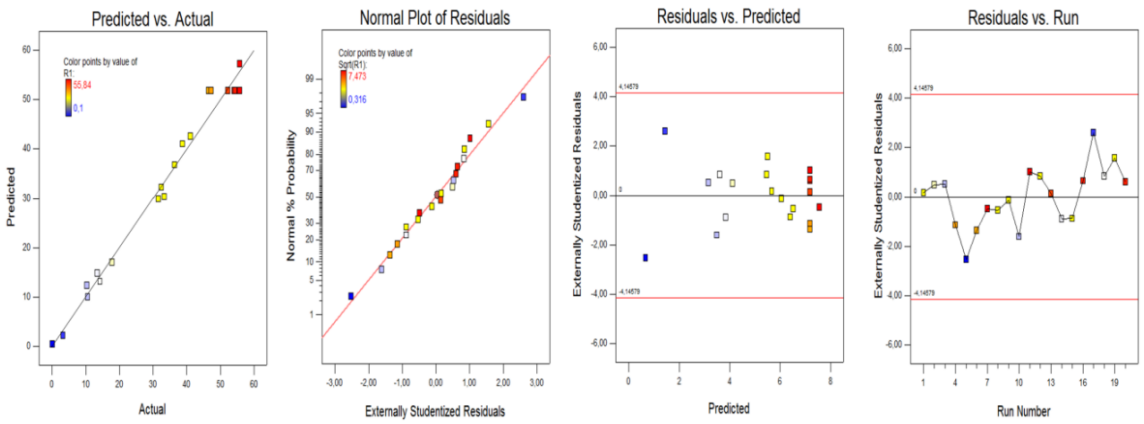


Fig. 5 All diagnostic plots of optimization $Ni^{2+}$ ions adsorption process using CCD: (a) actual and predicted; (b) normality; (c) studentized residuals and predicted; (d) studentized residuals and run values of $Ni^{2+}$ ions

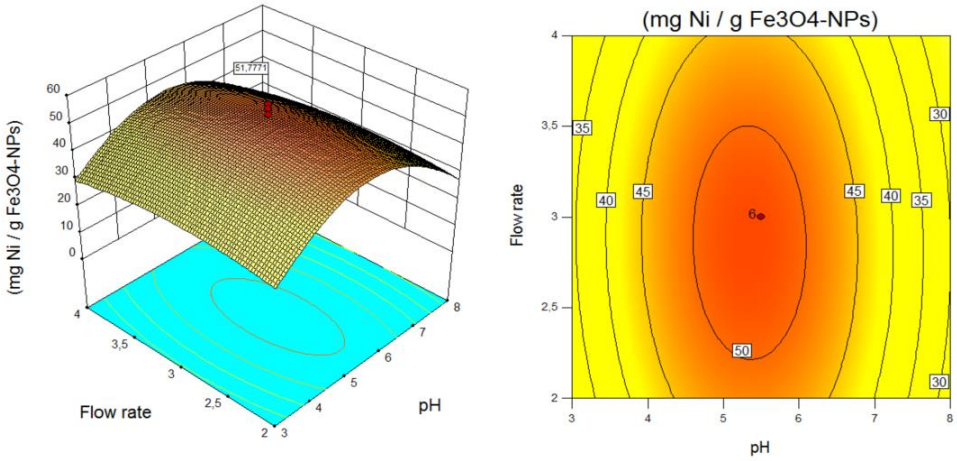


Fig. 6 Interactive effect of flow rate and pH

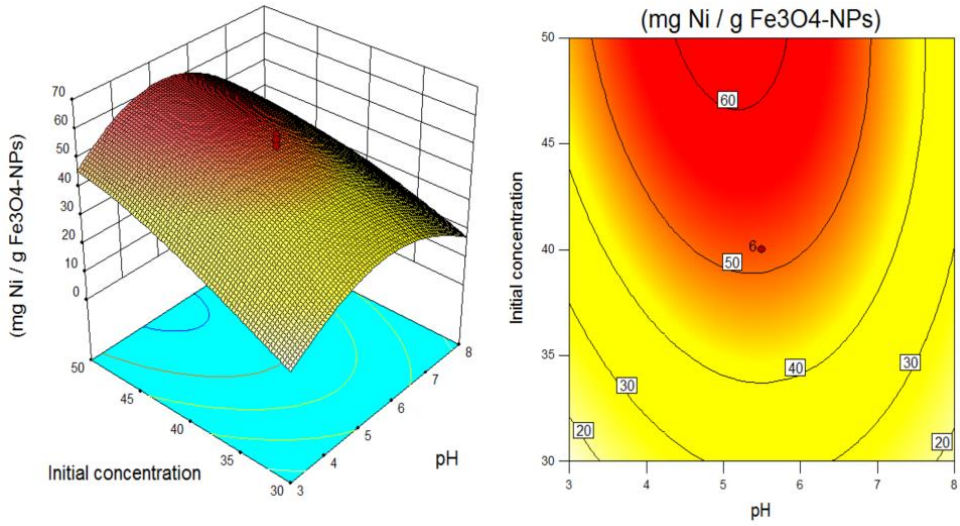


Fig. 7 Interactive effect of initial concentration and pH

### *3.2 Second-order polynomial model*

Test results of ANOVA that contain suggested second-order equation coefficients and model terms and a CCD programme for $Ni^{2+}$ ions adsorption on FBNM conditions are illustrated in Tables 1 and 2, respectively. As the Fisher test shows that the larger F-values and the smaller p-values indicate more meaningful the proposed model terms, it was

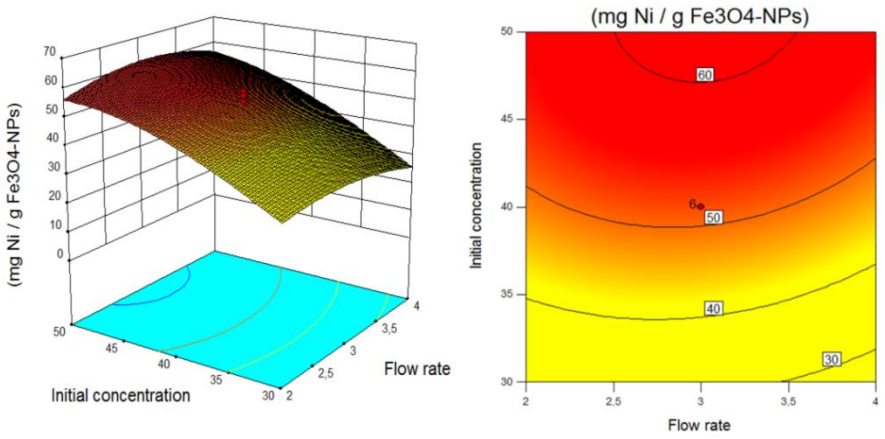


Fig. 8 Interactive effect of initial concentration and flow rate

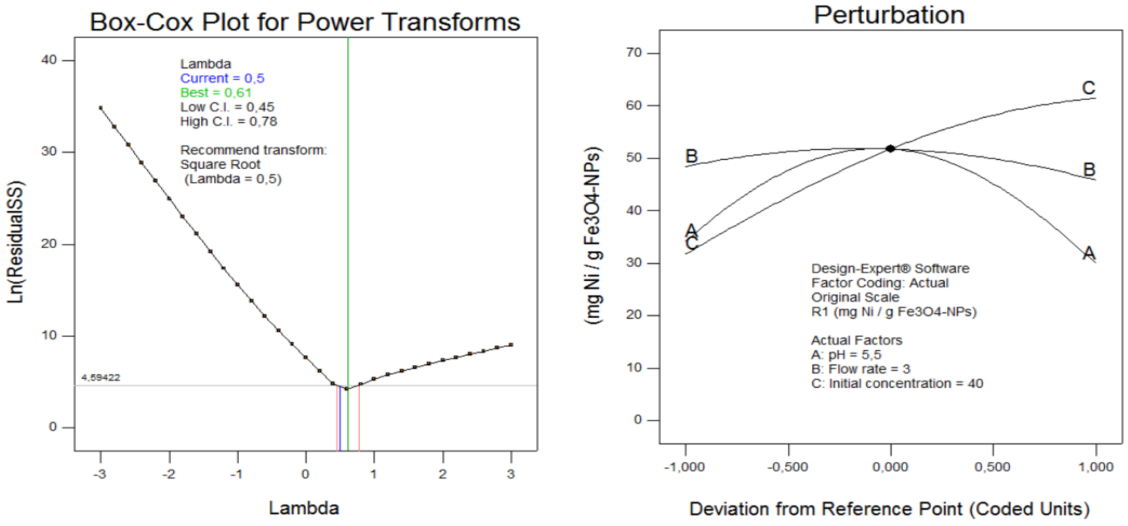


Fig. 9 Diagnostic plots: Box-Cox plot and perturbation plot for $Ni^{2+}$ ions removal, at the optimal conditions: (A) solution pH 5.5; (B) 2.5 mL $min^{-1}$ flow rate; (C) 49.5 mg $L^{-1}$ $Ni^{2+}$ ions initial concentration

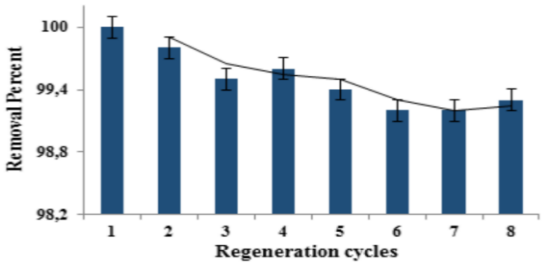


Fig. 10 Adsorption-desorption cycles of FBNM

tested by using ANOVA. While p-values less than 0.05, it was indicated a significant regression in 95% confidence level, in addition, F value is 95.55, indicating that the model is important. As "Prob > F" values less than 0.05 indicate model terms are significant as statistically. In this case $X_1$, $X_3$, $X_1X_3$, $X_1^2$, $X_2^2$ and $X_3^2$ values, are significant model terms but $X_2$, $X_1X_2$, $X_2X_3$ and values greater than 0.05 indicate the model terms are not significant. The "Lack-of-fit *p*-values" imply the "Lack-of-fit" is not significant relating to the pure error, it measures the fitness of the model ($p > 0.05$). In addition, number of experiments was enough to determine the effects of the independent variables for $Ni^{2+}$ ions adsorption on FBNM. This model goodness-of-fit was evaluated using determination coefficients ($R^2$) and determination adjusted coefficients (adj $R^2$). Since it defines the percentage of variability in the response, it is desirable to have a high $R^2$ value of the proposed model and this value should be greater than 0.75 for validity of the model (Ince and Kaplan Ince 2017). According to $R^2$ and adj $R^2$ values for the previously mentioned models were satisfactory. Because the model $R^2$ was obtained as 0.9886, it can be said that 98.86% of the model-predicted values matched the experimental adsorbed $Ni^{2+}$ ions values on FBNM. In addition, when the normal probability plot (Fig. 5) is examined, it can be said that residuals distribution is normal, and the model satisfies the assumptions of the ANOVA. They are reasonably compatible because the difference between the "Pred R-squared: 0.9373" and "Adj R-Squared: 0.9784" is less than 0.2. "Adeq precision" measures the signal to noise ratio and this ratio greater than 4 is desirable. The signal-to-noise ratio should be greater than 4 and it is measure by "Adeq precision". This value

obtained as 130.626 and it is indicating an adequate signal. Based on study results, used statistical model was adequate to predict of $Ni^{2+}$ ions levels and was fitted to second-order polynomial equation.

### 3.3 RSM analysis

Each parameter effect on $Ni^{2+}$ ions adsorption on FBNM and their interaction were presented in Figs. 6-8. Three-dimensional (3D) response surface graphs and two-dimensional (2D) contour plots are useful to determine response points including the maximum, middle and minimum and they were created according to quadratic model. Fig. 6 shows the 3D response surface and 2D contour plots of the influence of flow rate-pH on the adsorption efficiency of $Ni^{2+}$ ions on bio-nano adsorbent. While, it is evident that the $Ni^{2+}$ ions adsorption amount increased when pH increases until 5.5 ($p < 0.01$), after which an increase in metal uptake was observed. However, it was observed that $Ni^{2+}$ ions adsorption did not show a statistically significant increase or decrease tendency with flow rate change. These Fig. 6, 3D and 2D, showed that removal of $Ni^{2+}$ ions from the aqueous medium was strongly influenced by the pH. Solution pH influences the adsorbent surface charge, solubility of metal and protonation degree because of these properties solution pH significantly affects the metal ions adsorption on the adsorbents (Alizadeh *et al*. 2018).

On the other hand, it is clear that the amount of adsorbed $Ni^{2+}$ ions were increased when initial concentration ($p < 0.0001$) was increased up to 50 mg $L^{-1}$ (Fig. 7), when pH increases until 5.5 ($p < 0.01$). Based on ANOVA table, it was confirmed that these two variables had a significant effect on $Ni^{2+}$ ions adsorption on FBNM and the interaction of these two variables was statistically significant ($p < 0.05$).

Fig. 8 represents combined effect of initial concentration and flow rate on $Ni^{2+}$ ions removal at constant pH, adsorption of $Ni^{2+}$ ions increase with initial concentration increase, it was observed that increasing the flow rate was not have a significant effect on $Ni^{2+}$ ions adsorption on FBNM.

Panneerselvam *et al*. (2011), optimized some parameters as adsorbent dosage, pH, contact time, temperature and initial concentration for $Ni^{2+}$ ions removal by magnetic nanoparticle. It was determined that adsorption capacity was increased by the increasing of adsorbent dosage. This situation is available for contact time up to the saturation point. At the obtained optimum conditions adsorption capacity was calculated as 38.30 mg $g^{-1}$.

Ahmed and Fekry (2013) prepared nanoparticle, which coated with chitosan and used this nanoparticle to determine the heavy metals concentration in aqueous solutions. For identify the pH effect to $Ni^{2+}$ ions pH was studied in the range of 2-13. Up to pH 11, $Ni^{2+}$ ions current on the nanoparticles was increased.

Magnetic graphenes composite material was functionalized with amino and carried out to remove $Ni^{2+}$ ions from contaminated water. Batch adsorption technique was applied. $Ni^{2+}$ ions adsorption was increased by the pH increasing. Maximum adsorption was obtained at pH 6-7 and adsorption capacity was 22.07 mg $g^{-1}$ (Guo *et al.* 2014).

Co-precipitation method was used to obtain $Fe_3O_4$ nanoparticles at various sizes and by these nanoparticles heavy metals purified from waste water. Batch adsorption technique performed for purification. The parameters, which influenced the adsorption, were studied. The removal capacity was reached up to 99.9% with the 7 g of adsorbent dosage. For determination the optimum contact time from 2 h to 28 h were experimented and $Ni^{2+}$ ions adsorption was highly dependent on longer contact time. For determination the optimum temperature, in the range of 10-80°C was studied and it was found that the adsorption of $Ni^{2+}$ ions were increased up to 50°C. At pH 4 adsorption percentages of $Ni^{2+}$ ions were calculated as 88.5. At these optimum conditions $Ni^{2+}$ ions removal from waste water was calculated as 41.86 mg $L^{-1}$ (Shen *et al*. 2009).

Mondal *et al*. (2015) prepared air stable nanoparticles from cobalt sulphate using tetra butyl ammonium bromide as surfactant and sodium borohydride as reductant at room temperature. They indicated that the cobalt nanoparticles in aqueous sollutions were found to be effective catalysts for the degradation of toxic organic dyes such as methylene blue and rhodamine-B. Also, they found that recovered nanoparticles after removed toxic dyes could be recycled several times without loss of catalytic activity.

### 3.4 Desorption procedure and FBNM reuse studies

To recover the adsorbate after the use in any adsorption system and reuse is desirable situation because it reduces the cost and proves to be a qualified adsorbent. Bio-nano adsorbents can be damaged because of their sensitive structure during the process of desorption and reuse can destroy the bio-nanocomposite material. Reuse and desorption studies help to clarify the nature of the adsorption process. Some experimental studies were carried out to test used nano adsorbent, to understand whether desorption process is damaging. Firstly, about 25 mg of the bio-nanocomposite material was treated with $Ni^{2+}$ solution (40 µg $L^{-1}$, 50 mL) in a fixed-bed coloumn under optimum conditions that was determined using CCD. To elution of $Ni^{2+}$ ions from surface of FBNM, 0.1 mol $L^{-1}$ hydrochloric acid solution was used for desorption step. Separated elution solvent was measured to understand whether they contain $Ni^{2+}$ ions. It was observed that desorption solvents eluted 99% of the adsorbed $Ni^{2+}$ ions from the FBNM surface. After desorption, the $Ni^{2+}$ ions were adsorbed again on the FBNM surface based on previous optimum conditions. This procedure was repeated at least 8 times and the percentage of desorption was found to be greater than 98% (Fig. 10). The potential for repeated use of FBNM were found to be good. As highlighted, the FBNM good regenerate and reuse ability has considerably an advantage for application to removal of $Ni^{2+}$ ions from soft drinks.

### 3.5 Application to real samples

The applicability of the methodologies developed in this study has been tested for the real samples (Table 3). Under

Table 3 Removal of $Ni^{2+}$ ions using FBNM from various soft drinks

| Sample | Ni (μg $L^{-1}$) | | |
|---|---|---|---|
| | SA | Found | Removal (%) |
| Mineral water 1 | 0.0 | 4.8 ± 0.12 | |
| | 20 | 24.7 ± 1.4 | 99 |
| | 40 | 45.0 ± 2.2 | 100 |
| Mineral water 2 | 0.0 | 2.5 ± 0.2 | |
| | 20 | 22.3 ± 2.6 | 98.0 |
| | 40 | 43.1 ± 2.3 | 100 |
| Mineral water 3 | - | 4.6 ± 0.4 | |
| Mineral water 4 | - | 7.2 ± 0.2 | |
| Mineral water 5 | - | 3.1 ± 0.2 | |
| Fruit juice 1 | - | 2.2 ± 0.1 | |
| Fruit juice 2 | - | 1.8 ± 0.1 | |
| Fruit juice 3 | - | 1.7 ± 0.2 | |
| Fruit juice 4 | - | 1.7 ± 0.2 | |
| Fruit juice 5 | - | 2.7 ± 0.3 | |

*SA: Standard Addition

optimized conditions, experiments were performed with soft drink samples and samples spiked by $Ni^{2+}$ with various quantities (20 and 40 μg $L^{-1}$) were treated under the general procedure in optimized condition. The results revealed that acceptable removal percentage confirming the excellent performance of bio-nanocomposite material proposed for real samples.

## 4. Conclusions

It has been researched whether biosynthesized FBNM, which is an effective and reusable bionanomaterial, can eliminate $Ni^{2+}$ ions from the soft drink samples. In addition to the reusability potential of this bionanomaterial, experimental study design and multi-parameter optimization were carried out and the following results were obtained:

• To reach possible global optimal solution for maximizing the $Ni^{2+}$ ions removal from some soft drinks using biosynthesized FBNM with CCD optimization procedure was performed. To find out a suitable model leading to optimum outcome conditions (5.5 pH, 2.5 mL $min^{-1}$ flow rate and 49.5 mg $L^{-1}$ $Ni^{2+}$ ions initial concentration) a CCD method was identified to yield maximum $Ni^{2+}$ ions removal of 100%.

• The proposed mathematical model also provided a critical analysis for selected independent variables' interactive influences on $Ni^{2+}$ ions adsorption process.

• Obtained $R^2$ (0.9886) and adj $R^2$ (0.9784) values from the ANOVA were satisfactory. It can be said that 98.86% of the model-predicted values matched the experimental adsorbed $Ni^{2+}$ values on biosynthesized FBNM.

• Based on response surface plots (3D and 2D), $Ni^{2+}$ ions removal percentage from some soft drink samples were observed to increase with increasing pH up to 5.5.

• The maximum adsorption capacity of FBNM for $Ni^{2+}$ ions were calculated as 59.8 mg $g^{-1}$, in the experimental range of the variables.

• Data which obtained proposed three-factor CCD clearly confirmed that optimization is an effective approach for modeling the sorption process of $Ni^{2+}$ ions to understand the relationships among the independent and response variables and to maximize the process efficiency.

Conclusively, biosynthesized and used FBNM is a good candidate for removing the other pollutants because of adsorption capacity and reuse potential.

## References


Ahmed, R.A. and Fekry, A.M. (2013), "Preparation and characterization of a nanoparticles modified chitosan sensor and its application for the determination of heavy metals from different aqueous media", *Int. J. Electrochem. Sci*., **8**, 6692-6708.

Alizadeh, B., Delnavaz, M. and Shakeri, A. (2018), "Removal of Cd (II) and phenol using novel cross-linked magnetic EDTA/chitosan/$TiO_2$ nanocomposite", *Carbohydr. Polym*., **181**, 675-683. https://doi.org/10.1016/j.carbpol.2017.11.095.

Alp, H., Ince, M., Kaplan Ince, O. and Onal, A. (2019), "Adsorptive removal of Eriochrome Black-T using *Agaricus campestris*: Parameters optimization with response surface methodology", *Desalination Water Treat*., In Press.

Asgari, S., Fakhari, Z. and Berijani, S. (2014), "Synthesis and characterization of $Fe_3O_4$ magnetic nanoparticles coated with carboxymethyl chitosan grafted sodium methacrylate", *J. Nanostruct*., **4**(1), 55-63.

Bakraouy, H., Souabi, S., Digua, K., Dkhissi, O., Sabar, M. and Fadil, M. (2017), "Optimization of the treatment of an anaerobic pretreated landfill leachate by a coagulation-flocculation process using experimental design methodology", *Process Saf. Environ. Prot*., **109**, 621-630. https://doi.org/10.1016/j.psep.2017.04.017.

Balaz, M., Balazova, L., Kovacova, M., Daneu, N., Salayova, A., Bedlovicova, Z. and Tkacikova, L. (2019), "The relationship between precursor concentration and antibacterial activity of biosynthesized Ag nanoparticles", *Adv. Nano Res., Int. J*., **7**(2), 125-134. https://doi.org/10.12989/anr.2019.7.2.125.

Bhagawati, D., Thakur, S. and Karak, N. (2016), "Castor oil based hyperbranched polyester/bitumen modified fly ash nanocomposite", *Adv. Nano Res., Int. J*., **4**(1), 15-29. https://doi.org/10.12989/anr.2016.4.1.015.

Bhatnagar, A. and Minocha, A.K. (2010), "Biosorption optimization of nickel removal from water using *Punica granatum* peel waste", *Colloids Surf. B Biointerf*., **76**, 544-548. https://doi.org/10.1016/j.colsurfb.2009.12.016.

Boujelben, N., Bouzid, J. and Elouear, Z. (2009), "Adsorption of nickel and copper onto natural iron oxide-coated sand from aqueous solutions: Study in single and binary systems", *J. Hazard. Mater*., **163**(1), 376-382. https://doi.org/10.1016/j.jhazmat.2008.06.128.

Chen, B., Zhao, H., Chen, S., Long, F., Huang, B., Yang, B. and Pan, X. (2019), "A magnetically recyclable chitosan composite adsorbent functionalized with EDTA for simultaneous capture of anionic dye and heavy metals in complex wastewater", *Chem. Eng. J*., **356**, 69-80. https://doi.org/10.1016/j.cej.2018.08.222.

Chen, X., Zhang, Z., Li, X. and Shi, C. (2006), "Hollow magnetite spheres: Synthesis, characterization, and magnetic properties",

*Chem. Phys. Lett.*, **422**, 294-298. https://doi.org/10.1016/j.cplett.2006.02.082.

Chu, K.H. (2004), "Improved fixed bed models for metal biosorption", *Chem. Eng. J.*, **97**, 233-239. https://doi.org/10.1016/S1385-8947(03)00214-6.

Denkhaus, E. and Salnikow, K. (2002), "Nickel essentiality, toxicity, and carcinogenicity", *Crit. Rev. Oncol. Hematol.*, **42**(1), 35-56. https://doi.org/10.1016/S1040-8428(01)00214-1.

Ding, Y., Shen, S.Z., Sun, H., Sun, K., Liu, F., Qi, Y. and Yan, J. (2015), "Design and construction of polymerized-chitosan coated $Fe_3O_4$ magnetic nanoparticles and its application for hydrophobic drug deliver", *Mater. Sci. Eng. C*, **48**, 487-498. https://doi.org/10.1016/j.msec.2014.12.036.

Elbialy, N.S., Fathy, M.M. and Khalil, W.M. (2014), "Preparation and characterization of magnetic gold nanoparticles to be used as doxorubicin nanocarriers", *Phys. Med.*, **30**(7), 843-848. https://doi.org/10.1016/j.ejmp.2014.05.012.

Esalah, J. and Husein, M.M. (2008), "Removal of heavy metals from aqueous solutions by precipitation-filtration using novel organo-phosphorus ligands", *Sep. Sci. Technol.*, **43**, 3461-3475. https://doi.org/10.1080/01496390802219661.

Eticha, T. and Hymete, A. (2014), "Health risk assessment of heavy metals in locally produced beer to the population in Ethiopia", *J. Bioanal. Biomed.*, **6**, 65-68. https://doi.org/10.4172/1948-593X.1000114.

Fonseca, B., Teixeira, A., Figueiredo, H. and Tavares, T. (2009), "Modelling of the Cr (VI) transport in typical soils of the north of Portugal", *J. Hazard. Mater.*, **167**, 756-762. https://doi.org/10.1016/j.jhazmat.2009.01.049.

Garg, K.U., Kaur, M.P., Garg, V.K. and Sud, D. (2008), "Removal of nickel (II) from aqueous solutionby adsorption on agriculture waste biomass using a response surface methodological approach", *Bioresour. Technol.*, **99**(5), 1325-1331. https://doi.org/10.1016/j.biortech.2007.02.011.

Gu, H., Xu, K., Xu, C. and Xu, B. (2006), "Biofunctional magnetic nanoparticles for protein separation and pathogen detection", *Chem. Commun.*, **9**, 941-949. https://doi.org/10.1039/B514130C.

Guo, X., Du, B., Wei, Q., Yang, J., Hu, L., Yan, L. and Xu, W. (2014), "Synthesis of amino functionalized magnetic graphenes composite material and its application to remove Cr(VI), Pb(II), Hg(II), Cd(II) and Ni(II) from contaminated water", *J. Hazard Mater.*, **278**, 211-220. https://doi.org/10.1016/j.jhazmat.2014.05.075.

Haddad, P.S., Martins, T.M., D'Souza-Li, L., Li, L.M., Metze, K., Adam, R.L., Knobel, M. and Zanchet, D. (2008), "Structural and morphological investigation of magnetic nanoparticles based on iron oxides for biomedical applications", *Mater. Sci. Eng. C*, **28**(4), 489-494. https://doi.org/10.1016/j.msec.2007.04.014.

Hanafiah, M.A.K.M., Zakaria, H. and Ngah, W.S.W. (2010), "Base treated cogon grass (imperata cylindrica) as an adsorbent for the removal of Ni (II): Kinetic, isothermal and fixed-bed column studies", *Clean Soil Air Water*, **38**, 248-256. https://doi.org/10.1002/clen.200900206.

Hepziba Suganthi, S. and Kandasamy, R. (2017), "A novel single step synthesis and surface functionalization of iron oxide magnetic nanoparticles and thereof for the copper removal from pigment industry effluent", *Sep. Purif. Technol.*, **188**, 458-467. https://doi.org/10.1016/j.seppur.2017.07.059.

Hritcu, D., Popa, M.I., Popa, N., Badescu, V. and Balan, V. (2009), "Preparation and characterization of magnetic chitosan nanospheres", *Turk. J. Chem.*, **33**, 785-796.

Hu, J., Chen, G. and Lo, I.M.C. (2006), "Selective removal of heavy metals from industrial wastewater using maghemite nanoparticle: Performance and mechanism", *J. Environ. Eng.*, **132**(7), 702-715. https://doi.org/10.1061/(ASCE)0733-9372(2006)132:7(709).

Hu, P., Yu, L., Zuo, A., Guo, C. and Yuan, F. (2009), "Fabrication of monodisperse magnetite hollow spheres", *J. Phys. Chem. C*, **113**, 900-906. https://doi.org/10.1021/jp806406c.

Ince, M. (2014), "Comparision of Low-cost and eco-friendly adsorbent for adsorption of Ni(II)", *At. Spectrosc.*, **35**, 223-233.

Ince, M. and Kaplan Ince, O. (2017), "Box-Behnken design approach for optimizing removal of copper from wastewater using a novel and green adsorbent", *At. Spectrosc.*, **38**, 200-207.

Ince, M. and Kaplan Ince, O. (2019a), "Application of response surface methodological approach to optimize removal of Cr ions from industrial wastewater", *At. Spectrosc.*, **40**, 91-97.

Ince, M. and Kaplan Ince, O. (2019b), "Heavy metal removal techniques using response surface methodology: Water/wastewater treatment", *IntechOpen*, **2019**, 88915. https://doi.org/10.5772/intechopen.88915.

Ince, M., Kaplan Ince, O., Asam, E. and Onal, A. (2017), "Using food wastes biomass as effective adsorbents in water and wastewater treatment for Cu(II) removal", *At. Spectrosc.*, **38**, 142-148.

Kadirvelu, K., Thamaraiselvi, K. and Namasivayam, C. (2001), "Adsorption of nickel (II) from aqueous solution onto activated carbon prepared from Coirpith", *Sep. Purif. Technol.*, **124**(3), 497-505. https://doi.org/10.1016/S1383-5866(01)00149-6.

Kaplan Ince, O., Ince, M., Yonten, V. and Goksu, A. (2017), "A food waste utilization study for removing Lead(II) from drinks", *Food Chem.*, **214**, 637-643. https://doi.org/10.1016/j.foodchem.2016.07.117.

Kaplan Ince, O., Ince, M. and Onal, A. (2018), "Response Surface modeling for Pb(II) removal from alcoholic beverages using natural clay: Process optimization with Box-Behnken experimental design and determination by electrothermal AAS", *At. Spectrosc.*, **39**, 242-250.

Katsou, E., Malamis, S., Haralambous, K.J. and Loizidou, M. (2010), "Use of ultrafiltration membranes and aluminosilicate minerals for nickel removal from industrial wastewater", *J. Membr. Sci.*, **360**(1-2), 234-249. https://doi.org/10.1016/j.memsci.2010.05.020.

Landaburu-Aguirre, J., Pongracz, E., Peramaki, P. and Keiski, R.L. (2010), "Micellar-enhanced ultrafiltration for the removal of cadmium and zinc: Use of response surface methodology to improve understanding of process performance and optimization", *J. Hazard. Mater.*, **180**, 524-534. https://doi.org/10.1016/j.jhazmat.2010.04.066.

Lee, S.Y. and Harris, M.T. (2006), "Surface modification of magnetic nanoparticles capped by oleic acids: Characterization and colloidal stability in polar solvents", *J. Coll. Interf. Sci.*, **293**, 401-408. https://doi.org/10.1016/j.jcis.2005.06.062.

Li, G., Jiang, Y., Huang, K., Ding, P. and Chen, J. (2008), "Preparation and properties of magnetic $Fe_3O_4$-chitosan nanoparticles", *J. Alloys Compd.*, **466**, 451-456. https://doi.org/10.1016/j.jallcom.2007.11.100.

Liu, Z.L., Wang, H.B., Lu, Q.H., Du, G.H., Peng, L., Du, Y.Q., Zhang, S.M. and Yao, K.L. (2004), "Synthesis and characterization of ultrafine well-dispersed magnetic nanoparticle", *J. Magn. Magn. Mater.*, **283**(2-3), 258-262. https://doi.org/10.1016/j.jmmm.2004.05.031.

Liu, J., Liu, W., Wang, Y., Xu, M. and Wang, B. (2016), "A novel reusable nanocomposite adsorbent, xanthated $Fe_3O_4$-chitosan grafted onto graphene oxide, for removing Cu (II) from aqueous solutions", *Appl. Surf. Sci.*, **367**, 327-334. https://doi.org/10.1016/j.apsusc.2016.01.176.

Mak, S.Y. and Chen, D.H. (2005), "Binding and sulfonation of poly (acrylic acid) on iron oxide nanoparticles: A novel, magnetic, strong acid cation nano-adsorbent", *Macromol. Rapid Comm.*, **26**, 1567-1571. https://doi.org/10.1002/marc.200500397.

Malarkodi, C., Rajeshkumar, S., Paulkumar, K., Gnana Jobitha,

G., Vanaja, M. and Annadurai, G. (2013), "Biosynthesis of semiconductor nanoparticles by using sulfur reducing bacteria *Serratia nematodiphila*", *Adv. Nano Res., Int. J.*, **1**(2), 83-91. https://doi.org/10.12989/anr.2013.1.2.083.

Miralles, N., Valderrama, C., Casas, I., Martinez, M. and Florido, A. (2010), "Cadmium and lead removal from aqueous solution by grape stalk wastes: Modeling of a fixed-bed column", *J. Chem. Eng. Data*, **55**, 3548-3554. https://doi.org/10.1021/je100200w.

Mohan, D., Sarswat, A., Singh, V.K., Alexandre-Franco, M. and Pittman Jr., C.U. (2011), "Development of magnetic activated carbon from almond shells for trinitrophenol removal from water", *Chem. Eng. J.*, **172**, 1111-1125. https://doi.org/10.1016/j.cej.2011.06.054.

Mohsen-Nia, M., Montazeri P. and Modarress, H. (2007), "Removal of $Cu^{2+}$ and $Ni^{2+}$ from wastewater with a chelating agent and reverse osmosis processes", *Desalination*, **217**, 276-281. https://doi.org/10.1016/j.desal.2006.01.043.

Mondal, A., Mondal, A. and Mukherjee D. (2015), "Room-temperature synthesis of cobalt nanoparticles and their use as catalysts for Methylene Blue and Rhodamine-B dye degradation", *Adv. Nano Res., Int. J.*, **3**(2), 67-79. https://doi.org/10.12989/anr.2015.3.2.067.

Mondal, M., Dutta, M. and De, S. (2017), "A novel ultrafiltration grade nickel iron oxide doped hollow fiber mixed matrix membrane: Spinning, characterization and application in heavy metal removal", *Sep. Purif. Technol.*, **188**, 155-166. https://doi.org/10.1016/j.seppur.2017.07.013.

Pacheco, S., Medina, M., Valencia, F. and Tapia, J. (2006), "Removal of inorganic mercury from polluted water using structured nanoparticles", *J. Environ. Eng. ASCE.*, **132**, 342-349. https://doi.org/10.1061/(ASCE)0733-9372(2006)132:3(342).

Padmavathy, V., Vasudevan, P. and Dhingra, S.C. (2003), "Biosorption of nickel (II) ions on Baker's yeast", *Process Biochem.*, **38**(10), 1389-1395. https://doi.org/10.1016/S0032-9592(02)00168-1.

Pala, A., Serdar, O., Ince, M. and Onal, A. (2019), "Modeling approach with Box-Behnken design for optimization of Pb bioaccumulation parameters in *Gammarus pulex* (L., 1758)", *At. Spectrosc.*, **40**, 98-103.

Pan, B.C., Meng, F.W., Chen, X.Q., Pan, B.J., Li, X.T., Zhang, W.M., Zhang, X., Chen, J.L., Zhang, Q.X. and Sun, Y. (2005), "Application of an effective method in predicting breakthrough curves of fixed-bed adsorption onto resin adsorbent", *J. Hazard Mater.*, **124**, 74-80. https://doi.org/10.1016/j.jhazmat.2005.03.052.

Panneerselvam, P., Morad, N. and Tan, K.A. (2011), "Magnetic nanoparticle ($Fe_3O_4$) impregnated onto tea waste for the removal of nickel (II) from aqueous solution", *J. Hazard Mater.*, **186**(1), 160-168. https://doi.org/10.1016/j.jhazmat.2010.10.102.

Punjabi, K., Mehta, S., Yedurkar, S., Jain, R., Mukherjee, S., Kale, A. and Deshpande, S. (2018), "Extracellular synthesis of silver nanoparticle by *Pseudomonas hibiscicola* - mechanistic approach", *Adv. Nano Res., Int. J.*, **6**(1), 81-92. https://doi.org/10.12989/anr.2018.6.1.081.

Qin, B., Luo, H., Liu, G., Zhang, R., Chen, S., Hou, Y. and Luo, Y. (2012), "Nickel ion removal from wastewater using the microbial electrolysis cell", *Bioresour. Technol.*, **121**, 458-461. https://doi.org/10.1016/j.biortech.2012.06.068.

Qu, J., Song, T., Liang, J., Bai, X., Li, Y., Wei, Y., Huang, S., Dong, L. and Jin, Y. (2019), "Adsorption of lead (II) from aqueous solution by modified Auricularia matrix waste: A fixed-bed column study", *Ecotoxicol. Environ. Saf.*, **169**, 722-729. https://doi.org/10.1016/j.ecoenv.2018.11.085.

Serdar, O., Pala, A., Ince, M. and Onal, A. (2019), "Modelling cadmium bioaccumulation in Gammarus pulex by using experimental design approach", *Chem. Ecol.*, **35**(10), 922-936. https://doi.org/10.1080/02757540.2019.1670814.

Shanmugapriya, A., Ramammurthy, R., Munusamy, V. and Parapurath, S.N. (2011), "Optimization of ceric ammonium nitrate initiated graft copolymerization of acrylonitrile onto chitosan", *J. Water Resour. Prot.*, **3**(6), 380-386. https://doi.org/10.4236/jwarp.2011.36048.

Sharma, Y.C. and Srivastava, V. (2010), "Separation of Ni (II) ions from aqueous solutions by magnetic nanoparticles", *J. Chem. Eng. Data.*, **55**, 1441-1442. https://doi.org/10.1021/je900619d.

Sharma, R. and Singh, B. (2013), "Removal of Ni (II) ions from aqueous solutions using modified rice straw in a fixed bed column", *Bioresour. Technol.*, **146**, 519-524. https://doi.org/10.1016/j.biortech.2013.07.146.

Sharma, Y.C., Srivastava, V., Weng, C.H. and Upadhyay, S.N. (2009), "Removal of Cr (VI) from wastewater by adsorption on iron nanoparticles", *Can. J. Chem. Eng.*, **87**, 921-929. https://doi.org/10.1002/cjce.20230.

Shen, Y.F., Tang, J., Nie, Z.H., Wang, Y.D., Ren, Y. and Zuo, L. (2009), "Preparation and application of magnetic $Fe_3O_4$ nanoparticles for wastewater purification", *Sep. Purif. Technol.*, **68**, 312-319. https://doi.org/10.1016/j.seppur.2009.05.020.

Silva, V.A.J., Andrade, P.L., Silva, M.P.C., Bustamante, D.A., Valladares, L.D.L.S. and Albino Aguiar, J. (2013), "Synthesis and characterization of $Fe_3O_4$ nanoparticles coated with fucan polysaccharides", *J. Magn. Magn. Mater.*, **343**, 138-143. https://doi.org/10.1016/j.jmmm.2013.04.062.

Smara, A., Delimi, R., Chainet, E. and Sandeaux, J. (2007), "Removal of heavy metals from diluted mixtures by a hybrid ion-exchange/electrodialysis process", *Sep. Purif. Technol.*, **57**, 103-110. https://doi.org/10.1016/j.seppur.2007.03.012.

Supraja, N., Dhivya, J., Prasad, T.N.V.K.V. and David, E. (2018), "Synthesis, characterization and dose dependent antimicrobial and anticancerous efficacy of phycogenic (*Sargassum muticum*) silver nanoparticles against breast cancer cells (MCF 7) cell line", *Adv. Nano Res., Int. J.*, **6**(2), 183-200. https://doi.org/10.12989/anr.2018.6.2.183.

Teja, A.S. and Koh, P.Y. (2009), "Synthesis, properties, and application of magnetic iron oxide nanoparticles", *Progr. Cryst. Growth Charact. Mater.*, **55**, 22-45. https://doi.org/10.1016/j.pcrysgrow.2008.08.003.

Tsega, M. and Dejene, F.B. (2017), "Influence of acidic pH on the formulation of $TiO_2$ nanocrystalline powders with enhanced photoluminescence property", *Heliyon*, **3**(2), 1-16. https://doi.org/10.1016/j.heliyon.2017.e00246.

Volesky, B. (2001), "Detoxification of metal-bearing effluents: biosorption for the next century", *Hydrometallurgy*, **59**(2-3), 203-216. https://doi.org/10.1016/S0304-386X(00)00160-2.

Wang, Z., Liu, X., Lv, M. and Meng, J. (2010), "A new kind of mesoporous $Fe_7Co_3$/carbon nanocomposite and its application as magnetically separable adsorber", *Mater. Lett.*, **64**(10), 1219-1221. https://doi.org/10.1016/j.matlet.2010.02.055.

Yuwei, C. and Jianlong, W. (2011), "Preparation and characterization of magnetic chitosan nanoparticles and its application for Cu(II) removal", *Chem. Eng. J.*, **168**(1), 286-292. https://doi.org/10.1016/j.cej.2011.01.006.

Zhou, J., Wu, W., Caruntu, D., Yu, M.H., Martin, A., Chen, J.F., O'Connor, C.J. and Zhou, W.L. (2007), "Synthesis of porous magnetic hollow silica nanospheres for nanomedicine application", *J. Phys. Chem. C*, **111**(47), 17473-17477. https://doi.org/10.1021/jp074123i.

Zhou, S., Li, Y., Cui, F., Jia, M., Yang, X., Wang, Y., Xie, L., Zhang, Q. and Hou, Z. (2014), "Development of multifunctional folate-poly (ethylene glycol) chitosan-coated $Fe_3O_4$ nanoparticles for biomedical applications", *Macromol. Res.*, **22**, 58-66. https://doi.org/10.1007/s13233-014-2008-y.

Zinadini, S., Zinatizadeh, A.A., Rahimi, M., Vatanpour, V., Zangeneh, H. and Beygzadeh, M. (2014), "Novel high flux

antifouling nanofiltration membranes for dye removalcontaining carboxymethyl chitosan coated $Fe_3O_4$ nanoparticles", *Desalination*, **349**, 145-154. https://doi.org/10.1016/j.desal.2014.07.007.

*CC*